Understanding widely scattered traffic flows, the capacity drop, and platoons as effects of variance-driven time gaps

Martin Treiber,[1,*] Arne Kesting,[1,†] and Dirk Helbing[1,2,‡]
[1]*Dresden University of Technology, Andreas-Schubert-Str. 23, 01062 Dresden, Germany*
[2]*Collegium Budapest-Institute for Advanced Study, Szentháromság u. 2, H-1014 Budapest, Hungary*
(Received 30 August 2005; revised manuscript received 13 January 2006; published 31 July 2006)

We investigate the adaptation of the time headways in car-following models as a function of the local velocity variance, which is a measure of the inhomogeneity of traffic flow. We apply this mechanism to several car-following models and simulate traffic breakdowns in open systems with an on-ramp as bottleneck and in a closed ring road. Single-vehicle data and one-minute aggregated data generated by several virtual detectors show a semiquantitative agreement with microscopic and flow-density data from the Dutch freeway A9. This includes the observed distributions of the net time headways for free and congested traffic, the velocity variance as a function of density, and the fundamental diagram. The modal value of the time headway distribution is shifted by a factor of about 2 under congested conditions. Macroscopically, this corresponds to the capacity drop at the transition from free to congested traffic. The simulated fundamental diagram shows free, synchronized, and jammed traffic, and a wide scattering in the congested traffic regime. We explain this by a self-organized variance-driven process that leads to the spontaneous formation and decay of long-lived platoons even for a deterministic dynamics on a single lane.

DOI: 10.1103/PhysRevE.74.016123 PACS number(s): 89.40.−a, 05.60.−k, 05.70.Fh, 47.55.−t

I. INTRODUCTION

One of the open questions of traffic dynamics is a microscopic understanding of the observed wide variations in the time-headway distributions [1,2] that are closely related to the wide scattering of flow-density data in the congested regime [3,4], see, e.g., Refs. [5,6] for an overview. Apart from their wide variations, the average values of the time headways depend strongly on the traffic density. For congested traffic, the modal value, i.e., the value where the distribution has its maximum, is larger by a factor of about 2 compared to free traffic. Figure 1(a) shows a typical example obtained from single-vehicle detector data of the Dutch freeway A9 from Haarlem to Amsterdam.

With the increasing availability of single-vehicle data [1,2,7], further statistical properties of traffic became the subject of investigation such as the velocity variance as a function of the traffic density [8], or the distribution of the times-to-collision (TTC), which plays an important role for traffic safety [9,10].

In this paper, we therefore propose a variance-driven adaptation mechanism, according to which drivers increase their safety time gaps T when the local traffic dynamics is unstable or largely varying. This adaptation is, e.g., reflected in the empirically observed increase of the variation coefficient $V=\theta/\bar{v}$ and offers a safety-oriented interpretation of the capacity drop, i.e., the significant reduction of traffic flow when it becomes unstable [11–13].

Variance-driven time headways can also qualitatively explain the distribution of times-to-collision, which is surprisingly invariant with respect to density changes (compared to distance, time gap, or velocity distributions). Times-to-collision are, therefore, not only an interesting measure for traffic safety, but also a meaningful variable of behaviorally oriented traffic models based on the physical approach of invariants [14,15].

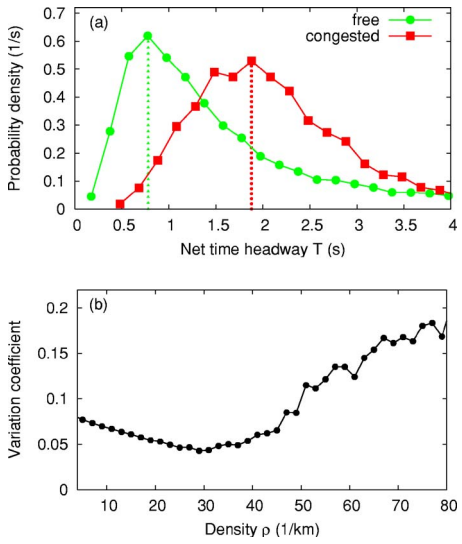

FIG. 1. (Color online) Empirical statistical properties of cars following any kind of vehicle obtained from single-vehicle data from the left lane of the Dutch freeway A9 at a detector cross section 1.0 km upstream of an on-ramp. (a) Net time headway according to Eq. (17); (b) variance coefficient V_n according to Eq. (2), as a function of the density. In (a) and (b), the data set for free traffic includes all single-vehicle data where the 1-minute average of velocities was above 20 m/s, and the traffic flow above 1000 vehicles/h. Congested traffic includes all data where the 1-minute average of the velocities was below 15 m/s.

*Electronic address: martin@mtreiber.de; URL: http://www.traffic-simulation.de
†Electronic address: kesting@vwi.tu-dresden.de
‡Electronic address: helbing1@vwi.tu-dresden.de; URL: http://www.helbing.org

The variance-driven increase of the safety time gap T may also be seen as an alternative to a frustration-driven increase of T after a long time in congested traffic [1,16–18]. Moreover, it potentially overcomes the criticism of traffic models with a fundamental diagram by Kerner [5], as it causes a pronounced platooning effect when traffic flow is perturbed or unstable. This guarantees a wide gap distribution which is the main prerequisite to reproduce the wide scattering of flow-density data in congested traffic [3].

Previous explanations of the wide scattering of flow-density data include stochastic effects [19,20], and sustained nonequilibrium states caused by dynamic instabilities such as stop-and-go traffic [16]. Stochastic terms are included in most cellular-automaton traffic models [21,22] and also in some car-following models, e.g., in the Gipps model [19] or in recent car-following models proposed by Kerner [23] or Wagner [24]. Another explanation of the scattering is based on the heterogeneity of vehicles (such as cars and trucks) and driving styles (such as defensive or aggressive) [12,25,26]. However, while all these effects can possibly account for the observed variations of time headways and times-to-collision, at least for a given traffic density, the scattering of flow-density data would be smaller than observed due to the averaging implied in aggregating single-vehicle data to, e.g., 1-minute data [4].

In the next section, we will introduce the mechanism of variance-driven time headways (VDT) in terms of a meta-model which can be applied to a wide range of car-following models. Section III introduces a general method to add fluctuations to car-following models. In Sec. IV, we apply the VDT mechanism to three microscopic traffic models and compare virtual-detector data directly with empirical findings. We found that *this simple mechanism can semiquantitatively explain all the microscopic and macroscopic empirical findings mentioned above*. In the concluding Sec. V, we discuss the effects of the VDT mechanism in terms of a spontaneous formation and decay of vehicle platoons, and point to applications in the field of traffic control and driver-assistance systems.

II. VARIANCE-DRIVEN ADAPTATION OF THE TIME HEADWAY

We will formulate the variance-driven time headways model in terms of a meta-model to be applied to any car-following model where the time headway T_0 for equilibrium traffic can be expressed by a model parameter or a combination of model parameters.

The basic assumption of the VDT is that smooth traffic flow allows for lower values of the time headway than disturbed traffic flow where the actual time headway

$$T = \alpha_T T_0 \tag{1}$$

is increased with respect to T_0 by a factor $\alpha_T \geqslant 1$. Furthermore, we characterize disturbed traffic flow (such as stop-and-go traffic) by relatively high values of the velocity differences between following vehicles. Since a driver in vehicle α must assess the heterogeneity of traffic flow *in situ*, any measure for the heterogeneity may only depend on the immediate environment. One of the simplest measure satisfying this requirement is the *local variation coefficient*

$$V_n = \frac{\sqrt{\theta_n}}{\bar{v}_n}, \tag{2}$$

where the local velocity average

$$\bar{v}_n = \frac{1}{n}\sum_{i=0}^{n-1} v_{\alpha-i}, \tag{3}$$

and the local variance

$$\theta_n = \frac{1}{n-1}\sum_{i=0}^{n-1} (v_{\alpha-i} - \bar{v}_n)^2 \tag{4}$$

are calculated from their own velocity v_α and the velocities of the $(n-1)$ predecessors $(\alpha-i)$, $i=1,\ldots,n-1$. For the sake of simplicity we will skip the vehicle index α here, and in all subsequent equations. In this work, we will set $n=5$ in most cases, i.e., the adaptation of the drivers is assumed to depend on the own velocity and the velocities of the four nearest vehicles in front.

This quantity can be empirically determined if single-vehicle data are available. Figure 1(c) shows an example for the Dutch freeway A9 between Haarlem and Amsterdam. Notice that, for a given local density ρ, the variation coefficient $V_n = \sqrt{A}$ is related to the variance prefactor $A(\rho)$ introduced in the macroscopic gas-kinetic-based traffic (GKT) model [8].

It is obvious that the multiplicator α_T in Eq. (1) should increase monotonously with the variation coefficient and that it is restricted to a value of about 2 (which means a doubling of the time gap under very unsteady traffic conditions). One of the simplest relations satisfying this is a linearly increasing function with a cutoff such as

$$T = \alpha_T T_0 = [\min(1 + \gamma V_n, \alpha_T^{\max})] T_0. \tag{5}$$

Here, $\alpha_T^{\max}$ denotes the maximum multiplication factor for the time headway found for traffic flows of maximum unsteadiness, and γ the sensitivity of the time headway to increasing velocity variations.

In summary, the VDT mechanism is completely defined by Eq. (5), reflecting that the necessary time headway for safe driving depends on the velocity variance of the surrounding traffic. This proposition of variance-driven time headways (VDT) can be applied to any time-continuous car-following model in which the time headway can be expressed by a model parameter or a combination of parameters. Some examples are the optimal-velocity model (OVM) [27], the velocity-difference model (VDIFF) [28], the intelligent-driver model (IDM) [29], or the Gibbs model [19].

The VDT has three parameters, namely the number n of vehicles used to determine the local velocity variance, the maximum multiplication factor $\alpha_T^{\max}$ by which the time headway is increased compared to perfectly smooth traffic, and the sensitivity γ (see Table I). For the special case $n=2$, the VDT acceleration depends only on the velocity difference to the immediate predecessor, i.e., one obtains a simple car-

TABLE I. (Color online) Model parameters of the VDT approach used throughout this paper for all simulated car-following models. The strength of the acceleration noise (cf. Sec. III) was set to 0.1 m^2/s^3.

Parameter	Value
Number n of vehicles for determining θ	5
Time-headway multiplication factor in unsteady traffic $\alpha_T^{\max}$	2.2
Sensitivity γ	4.0

following model depending only on the immediate predecessor (at least, if this is the case for the underlying car-following model). However, the model yields more realistic results for a larger number of vehicles, therefore we will assume $n=5$ in all simulations. Larger values for n will not change the dynamics significantly.

The parameters $\alpha_T^{\max}$ and γ can be determined from empirical data of the time-headway distribution for free and congested traffic, and from the observed maximum variation coefficient $V_n^{\max}$. Figure 1 shows these data for the Dutch freeway A9 from Haarlem to Amsterdam [1]. Figure 1(a) shows that the locations of the maxima (modal values) of the time-headway distributions for free and congested traffic differ by a factor of about 2. We therefore set $\alpha_T^{\max}=2.2$ in all simulations. The parameter γ can be determined by the approximate relation

$$\gamma \approx \frac{\alpha_T^{\max}-1}{V_n^{\max}}. \tag{6}$$

From Fig. 1(c) we see that $V_n^{\max}$ is slightly below 0.2, so we set $\gamma=4$ in all simulations.

III. ACCELERATION NOISE

Fluctuating forces in microscopic traffic models are used to globally describe all influences that are not modeled explicitly such as imperfect estimation capabilities [14], lack of attention, or simply the fact that drivers do not always react identically to a given traffic situation. Fluctuation terms are part of nearly all cellular automata (the most popular example being the Nagel-Schreckenberg model [21] and models derived from it [30]), but are less commonly used in time-continuous car-following models.

Since the VDT is essentially based on fluctuations of the velocity, it is to be expected that purely deterministic underlying models yield unrealistic results due to the lack of an initial source triggering the fluctuations. Therefore, we consider additional acceleration fluctuations when applying the VDT to a deterministic model.

For simplicity, we will just add a white (independent and δ-correlated) noise term [31] to the deterministic car-following acceleration $a_\alpha^{(\mathrm{det})}$ according to

$$\dot{v}_\alpha = a_\alpha^{(\mathrm{det})}(t) + \sqrt{Q}\xi_\alpha(t). \tag{7}$$

Here, Q denotes the fluctuation strength (cf. Table I), and the white noise $\xi(t)$ is assumed to be unbiased and δ correlated,

$$\langle \xi_\alpha \rangle = 0, \quad \langle \xi_\alpha(t)\xi_\beta(t')\rangle = Q\delta_{\alpha\beta}\delta(t-t'). \tag{8}$$

The Kronecker symbol $\delta_{\alpha\beta}$ is 1, if $\alpha=\beta$ and zero otherwise, while the Dirac function $\delta(t)$ is defined by $\int_{-\infty}^{\infty}\delta(t')dt'=1$ and $\delta(t)=0$ for $t\neq 0$. To clarify the effects of the fluctuation term on the velocity, we note that

(i) in the absence of a deterministic acceleration, Eq. (7) leads to velocities $v_\alpha(t)$ fluctuating stochastically around the initial velocity $v_\alpha(t_0)$ with a linearly-in-time increasing variance (random walk),

$$\theta_\alpha = Q(t-t_0), \tag{9}$$

(ii) under the linearized deterministic (relaxational) dynamics $a_\alpha^{\mathrm{det}}=(v_0-v)/\tau$ (where v_0 is the desired velocity, v the actual velocity, and τ the acceleration relaxation time), the velocity variance of the stationary state is given by the fluctuation-dissipation result [32]

$$\theta = Q\tau. \tag{10}$$

In the explicit numerical velocity update from time t to $t+\delta t$,

$$v_\alpha(t+\delta t) = v_\alpha(t) + a_\alpha^{\mathrm{det}}\delta t + \eta_t\sqrt{Q\delta t}, \tag{11}$$

we have implemented the stochastic term by the additive contribution $\eta_t\sqrt{Q\delta t}$, where the $\{\eta_t\}$ are statistically independent realizations of Gaussian distributed random numbers with zero mean and unit variance [32].

The velocity update according to (11) is numerically consistent in the stochastic sense. More precisely, we have considered the numerical velocity distribution function $F^{\mathrm{num}}(v,t)=\mathrm{Prob}[v_\alpha(t)\leqslant v]$ obtained from many simulations with different seeds for the pseudorandom number generator at a given time t. We have then compared the numerical distribution function with the theoretical distribution $F(v,t)=\int_{-\infty}^{v}dv'P(v',t)$ where $P(v,t)$ is the solution to the Fokker-Planck equation corresponding to Eq. (7),

$$\frac{\partial P(v_\alpha,t)}{\partial t} + a_\alpha^{(\mathrm{det})}\frac{\partial P}{\partial v_\alpha} = \frac{Q}{2}\frac{\partial^2 P}{\partial v_\alpha^2}. \tag{12}$$

It turned out that the deviations between $F^{\mathrm{num}}(v,t)$ and $F(v,t)$ are of the order $O(\delta t)$. Notice that this means that, for sufficiently small time steps δt, the result is independent from δt and agrees with the analytic solution to the stochastic differential equation (7).

We have checked this for the random walk and linear relaxation scenarios mentioned above and found a very good agreement between the numerical results from the update scheme (11) and the analytical results (9) and (10), respectively. (See Ref. [31] for a more detailed discussion.)

In summary, Eqs. (7)–(11) contain only a single model parameter Q, which can be considered as a general approach to add acceleration noise to time-continuous deterministic car-following models, where this is of interest. Clearly, δ-correlated noise terms are unrealistic in many respects. Therefore, we have also simulated more realistic time-correlated and multiplicative noise, which clearly describes the human origins of acceleration noise better [14], but we found no qualitative difference.

IV. SIMULATION RESULTS

In the following, we will apply the VDT to three car-following models, namely the intelligent-driver model (IDM) [29], the optimal-velocity model (OVM) [27], and the velocity-difference model [28], which augments the OVM by a term proportional to the velocity difference. We will also simulate heterogeneous traffic consisting of a mixture of these models.

For the purpose of reference and in order to discuss the coupling to the VDT, we shortly present the model equations, i.e., the acceleration functions, of these models.

The IDM acceleration $\dot{v}_{\mathrm{IDM}}(s,v,\Delta v)$ of a vehicle as a function of the (net) distance s to the predecessor, the velocity v, and the velocity difference Δv (positive when approaching) is given by

$$\dot{v}_{\mathrm{IDM}} = a\left[1 - \left(\frac{v}{v_0}\right)^4 - \left(\frac{s^*}{s}\right)^2\right] \tag{13}$$

with the desired dynamical distance

$$s^* = s_0 + vT + \frac{v\Delta v}{2\sqrt{ab}}. \tag{14}$$

The acceleration of the velocity-difference models is given by

$$\dot{v}_{\mathrm{OVM}} = \frac{v_{\mathrm{opt}} - v}{\tau} - \lambda\Delta v, \tag{15}$$

where $\lambda = 0$ for the OVM and the optimal velocity is given by

$$v_{\mathrm{opt}}(s) = \frac{v_0}{2}\left[\tanh\left(\frac{s}{L} - \beta\right) - \tanh(-\beta)\right]. \tag{16}$$

The coupling (1) of the VDT to the IDM is simple, since the desired time headway T is already an IDM parameter. We used $T = T_0 = 0.7$ s as minimum value which can be increased up to $T = 1.54$ s corresponding to $\alpha_T^{\max} = 2.2$ (cf. Table I). To find an appropriate coupling of the VDT to the OVM and VDIFF models, we note that the parameter L defines a typical interaction range and, consequently, the desired time headway $s/v_{\mathrm{opt}}(s)$ is essentially proportional to L/v_0 in these models. Therefore, we coupled the VDT to the OVM and the VDIFF models by setting $L = L_0\alpha_T$ with α_T according to Eq. (5).

We point out that these three example models differ in their dynamical properties. Consequently, the dynamics of the related VDT model is expected to depend to some degree on these models as well. However, we have also simulated models like the OVM in order to show that our VDT mechanism works also in combination with very simple models. To compare the quality of the VDT with detailed models such as that one proposed by Kerner [23], we favor the use of the IDM as underlying model. In order to distinguish between freely moving and following vehicles, we need at least two vehicle types (cars and trucks) with different desired velocities v_0. For all models, we have set $v_0 = 35$ m/s for cars, and $v_0 = 25$ m/s for trucks and simulated a truck percentage of 20%. For comparison, we have also performed simulations with identical vehicles of the type car. Notice that v_0 is a common parameter of all three models. Because we want to introduce as little complexity as possible, we did not distinguish cars and trucks with respect to other parameters. Particularly, the equilibrium time headway of stationary traffic was set to be the same for both vehicle types. Furthermore,

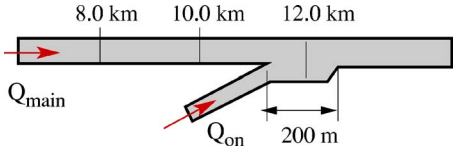

FIG. 2. (Color online) Simulated infrastructure and positions of virtual detectors. The units of locations are measured in kilometers.

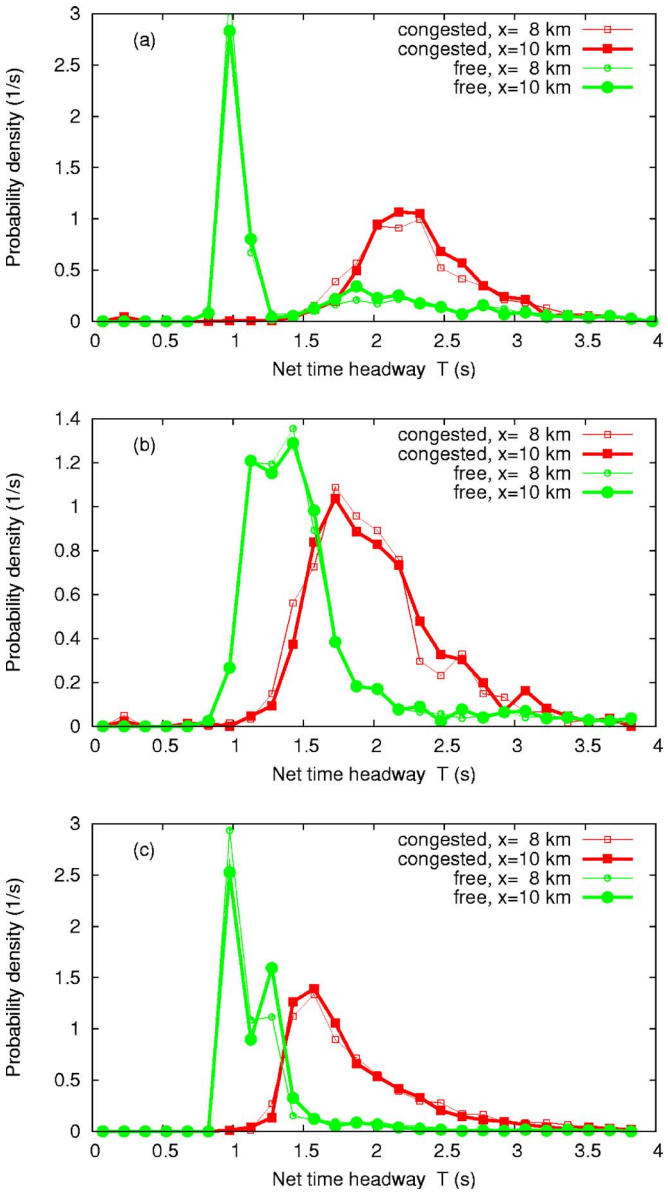

FIG. 3. (Color online) Distribution of the net time headways of cars following any kind of vehicle (cars or trucks) obtained from single-vehicle data of virtual detectors at various positions for simulations of the VDT with (a) the IDM; (b) the OVM; (c) the VDIFF model.

we used the same vehicle length $l_{veh}=5$ m for both vehicle types in all simulations.

The remaining IDM parameters are the minimum gap $s_0=3$ m, the acceleration $a=1$ m/s^2, and the comfortable deceleration $b=1.5$ m/s^2. For the OVM, we used the relaxation time $\tau=0.4$ s and the parameter β of the optimal-velocity relation to $\beta=1$. Furthermore, we set the minimum interaction length $L_0=13$ m for cars and $L_0=10$ m for trucks. Thus, the effective minimum time headway is about the same for both types. [Note that, according to Eq. (5), the actual interaction length $L=\alpha_T L_0$ is generally larger than L_0.] For the VDIFF, we used the same values for v_0, L_0, and β as for the OVM. Furthermore, we used $\tau=2$ s and the sensitivity coefficient $\lambda=1$ s^{-1}. For all models, we set the fluctuation strength $Q=0.1$ m^2/s^3. For comparison, we simulated also the deterministic VDT-IDM for which the fluctuation strength is $Q=0$, and the IDM without VDT modifications. The parameters were chosen such that the traffic dynamics was comparable to the Dutch freeway A9 freeway data with respect to the form of the fundamental diagram, capacity, and stability.

We have simulated a single-lane road section of total length 15 km with an on-ramp of length $L_{rmp}=200$ m located at $x_{rmp}=12$ km (Fig. 2) from which a constant flow of 400 vehicles/h merges to the main road. To keep matters simple, we have avoided explicit modeling of the merging of ramp vehicles to the main road. Instead, we have inserted the ramp vehicles centrally into the largest gap within the 200 m long ramp section. In order to generate a sufficient velocity perturbation in the merge area, the speed of the accelerating on-ramp vehicles at the time of insertion was assumed to be 50% of the velocity of the respective front vehicle. It turned out that the perturbations induced by the slower merging vehicles were crucial: When simulating merges with the same velocity as the main road vehicles, the onset of traffic breakdown was markedly delayed indicating the role of perturbations for traffic optimization (see Sec. V below).

We initialized the simulations with very light traffic of density $\rho=3$ vehicles/km vehicles/km and an initial velocity of 100 km/h. The details of the initial conditions, however, are not relevant unless they lead to an immediate breakdown of traffic flow. To generate congestion, we have increased the inflow of vehicles to the main lane linearly from 300 vehicles/h at $t=0$ s to 3000 vehicles/h at $t=2400$ s. Afterwards, we decreased the inflow linearly to 300 vehicles/h until $t=4800$ s. In case the inflow exceeded capacity, we delayed the insertion of new vehicles at the upstream boundary.

The update time step of the numerical integration scheme was $\delta t=0.05$ s for all models. Runs with smaller time steps yielded essentially the same results. In order to show that on-ramp perturbations are not necessary and acceleration fluctuations alone are sufficient to trigger a traffic breakdown, we have also simulated a closed system (ring road) of 15 km circumference, where the control parameter is the traffic density rather than the inflow (see Sec. IV C and Fig. 7).

A. Time-headway distribution

Empirical investigations of single-vehicle data have shown that the distributions of net time headways differ markedly in free and congested traffic situations [1,7], see Fig. 1.

To enable direct comparisons with experimental work, we have implemented virtual detectors at $x=8$ km and 10 km (cf. Fig. 2) recording the passage time t_α, type (car or truck) and velocity v_α of each vehicle α crossing the detector. We estimated the net time headway T_α by the time interval between the passage of the rear bumper of the preceding vehicle $(\alpha-1)$ and the front bumper of the vehicle under consideration,

$$T_\alpha = t_\alpha - t_{\alpha-1} - \frac{l_{\alpha-1}}{v_{\alpha-1}}. \tag{17}$$

Figure 3 shows the simulated distribution of T_α for the faster vehicle type (cars following any vehicle type) separately for free traffic ($v_\alpha > 15$ m/s) and congested traffic ($v_\alpha \leqslant 12$ m/s). We have obtained the following main results:

(i) The modal value (location of the maximum of the probability density) of the time headway is markedly higher (about 2 times as high for the VDT-IDM) in congested traffic compared to free traffic.

(ii) The values for T_α form a broad and asymmetrical distribution.

(iii) The different underlying models, particularly deterministic and stochastic variants, yielded qualitatively the same results. Remarkably, the velocity variance depends only weakly on the noise, while the peaks of the time-headway distributions become much sharper without noise [Fig. 4(a)]. Obviously, the role of the noise is to trigger the variance-driven dynamics.

Notice that the VDT only prescribes that the time headway increases with the variance. The dependence of the variance (and thus the average time headway) on the traffic situation results from the traffic dynamics. Moreover, all statistical data were obtained from identical vehicles (the cars). Since all cars have the same unique equilibrium relation between velocity and net distance s, the bimodal distributions are an interesting result, particularly for the deterministic case.

Nevertheless, the peaks of the simulated distributions are higher and sharper that those in the empirical data (cf. Fig. 1) The lacking quantitative agreement in this case can be explained by the wide variation of individually preferred time headways of drivers, i.e., in the variations of the driving style [4], which was neglected in our simulation for reasons of simplicity. To test this assumption, we have simulated a mix of all three models. The resulting time-headway distribution for congested traffic and the variance as a function of the density reproduces the observed data nearly quantitatively as shown in Fig. 5. For the sake of simplicity, we will, however, not incorporate a mix of several models in the rest of this work.

The question arises whether the above effects arise genuinely due to the VDT mechanism, or if they can be reproduced by heterogeneous traffic or noise alone. To distinguish the effects of the different influencing factors, we simulated the VDT mechanism for identical vehicles of type car [Fig. 4(b)], and the IDM without VDT and noise for the 80% to

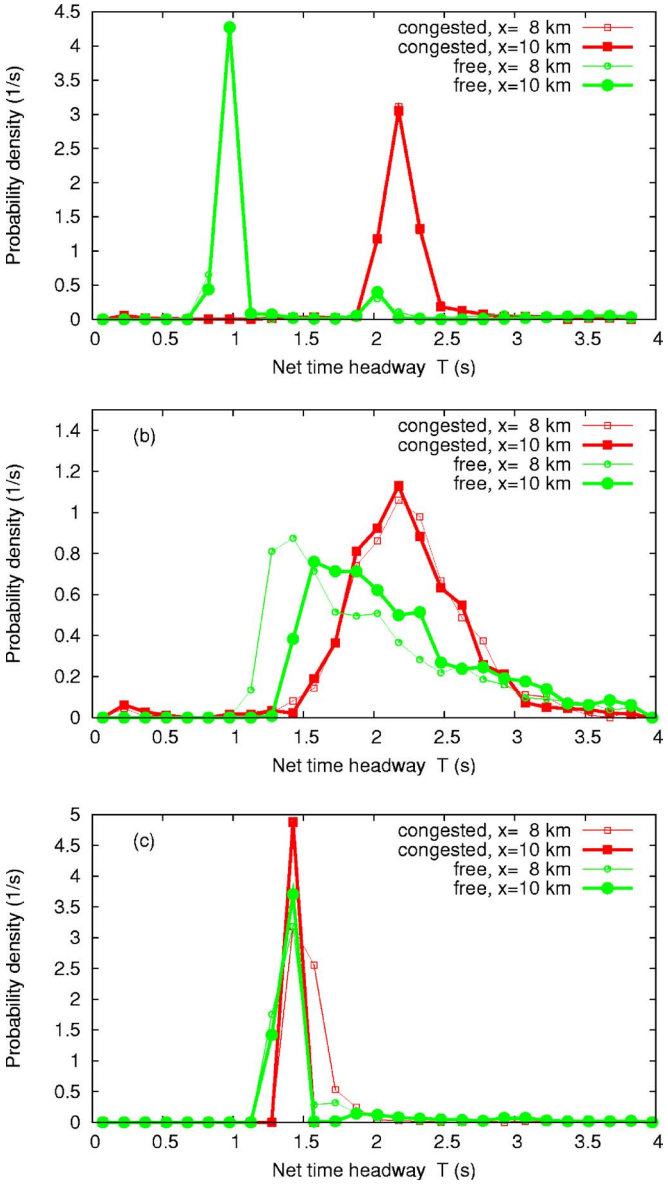

FIG. 4. (Color online) Distribution of the net time headways of cars for (a) the deterministic VDT-IDM with cars and trucks; (b) the stochastic VDT-IDM with only one vehicle type (cars); (c) the IDM with cars and trucks, but without VDT modifications.

20% mixture of cars and trucks [Fig. 4(c)]. While the separation of the time headways for free and congested traffic remained valid for VDT simulations with identical vehicles, simulations of the IDM for heterogeneous traffic but without VDT could not reproduce different time gap distributions before and after the breakdown of traffic [Fig. 4(c)].

B. Flow-density diagram

The flow-density diagram, also called the fundamental diagram, reveals several statistical and dynamical properties of traffic flow.

(i) The reverse-λ shape indicates the hysteresis phenomenon between free and congested traffic (capacity drop),

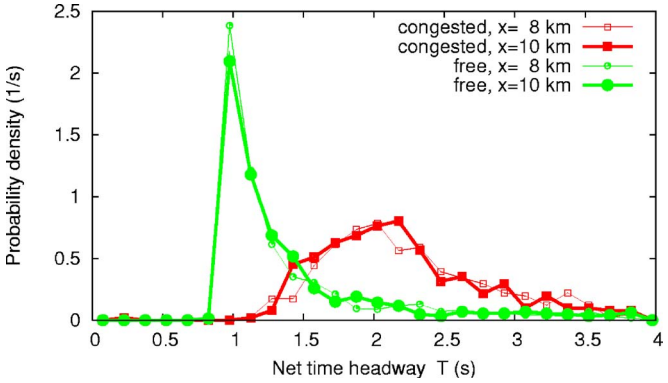

FIG. 5. (Color online) Distribution of time headways for the VDT with a mix of 1/3 IDM, 1/3 OVM, and 1/3 VDIFF vehicles (truck percentage 20% in each model).

(ii) the wide scattering in the congested region is a signature of synchronized flow [3],

(iii) regions with nonzero density but nearly zero flow indicate traffic jams.

Figure 6 shows that all three aspects of traffic dynamics can be simulated with the VDT. Remarkably, widely scattered flow-density data are also observed without noise [Fig. 6(b)]. To illustrate the influence of the on-ramp perturbation, we have introduced a sustained velocity perturbation in all simulations of Sec. IV and in Figs. 6(a) and 6(b) by letting accelerating ramp vehicles merge with only one-half the velocity of the vehicles on the main road. In simulations where the ramp vehicles entered with the speed of the vehicles on the main road, we observed a markedly delayed traffic breakdown occurring only after a traffic-flow peak near 3000 vehicles/h instead of 2500 vehicles/h, cf. Fig. 6(c). The subsequent breakdown, however, was more severe showing not only synchronized traffic but also jammed traffic with nearly vanishing flows. Eliminating the noise term alone had a smaller effect.

C. Simulation of closed systems

Without any perturbations (neither road inhomogeneities nor perturbations in the initial or boundary conditions nor acceleration noise) the VDT mechanism would lead to breakdowns only when the flow is approaching the static capacity (about 3000 vehicles/h for the VDT-IDM with the parameter set used in this paper). Notice that this unrealistically high value for the maximum flow is never observed in reality since perturbations of the flow, road inhomogeneities, and noise are always present on real roads. In order to check if acceleration noise alone can significantly lower this threshold we have also simulated a 15 km long closed ring road. This provides a simple system with less ad-hoc assumptions and allows to answer the question to which degree the statistical properties of the VDT mechanism are different in open and closed systems.

Figure 7 shows the results for simulations of traffic densities ranging from $\rho=15$ vehicles/km to $\rho=40$ vehicles/km. Comparing the fundamental diagram 7(a) with that of the corresponding open system 6(a) shows es-

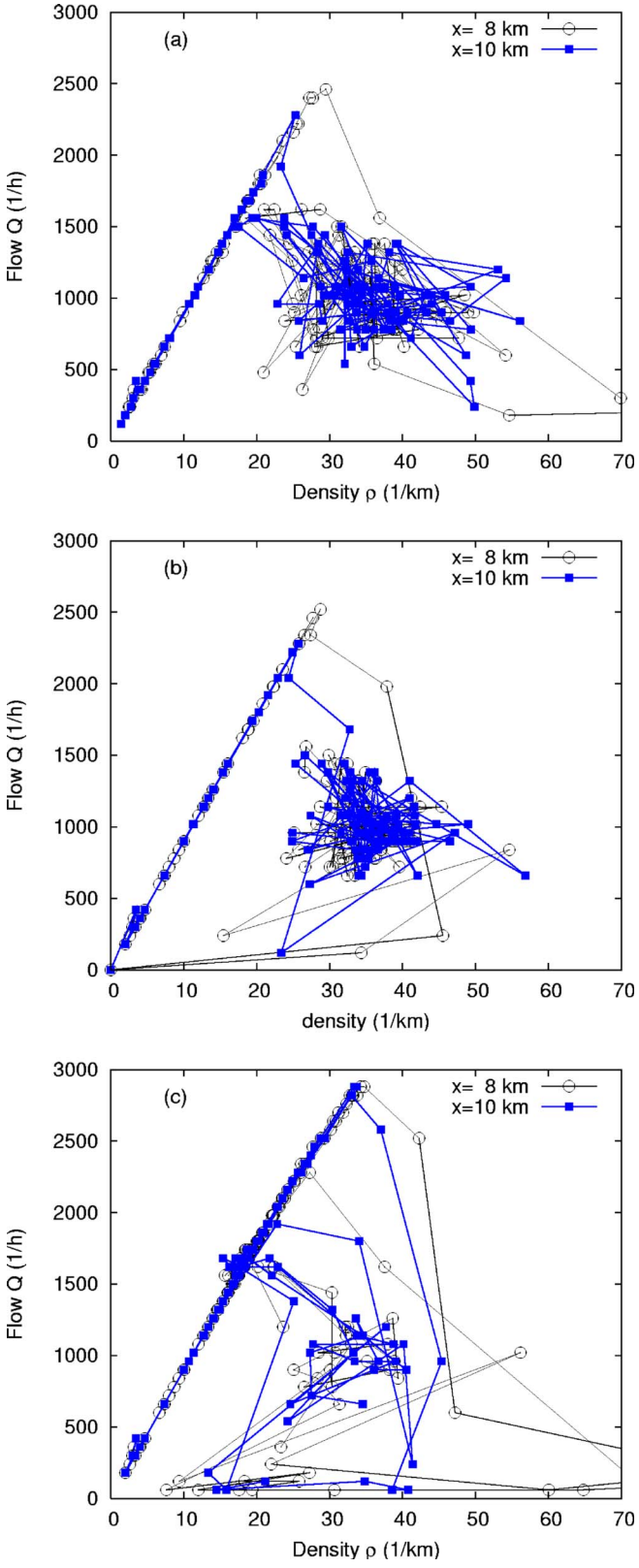

FIG. 6. (Color online) Simulated flow-density data of the VDT applied to the IDM at two virtual detectors with a sampling interval of $T_{aggr}=60$ s (a) with fluctuations; (b) without fluctuations; (c) without fluctuations and on-ramp vehicles merging with the speed of the vehicles on the main road rather than one-half of it as in (a) and (b).

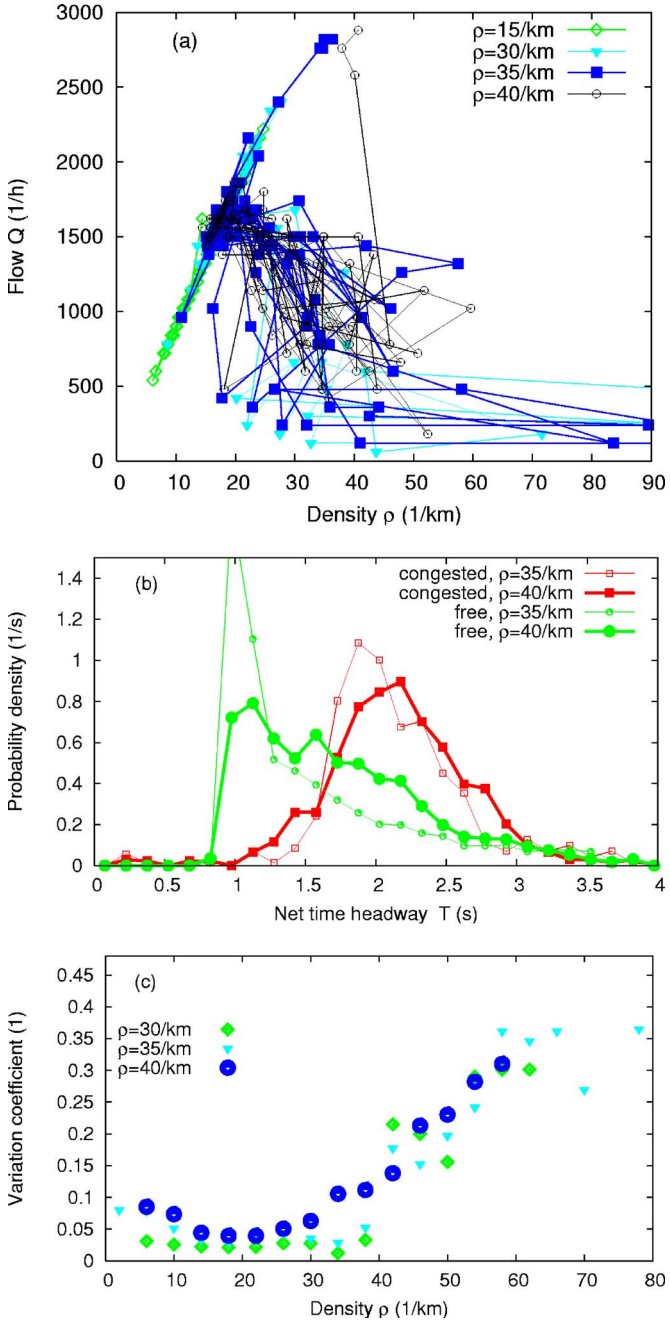

FIG. 7. (Color online) Simulation of a closed ring road with the stochastic VDT mechanism using the IDM. (a) Fundamental diagram; (b) time-headway distribution; (c) variation coefficient V_n for several densities as indicated.

sentially the same statistical properties for a density of $\rho=40$ vehicles/km. In both cases, the wide erratic scattering indicates synchronized traffic. In contrast, the large maximum densities of the diagrams for $\rho=30$ vehicles/km indicate regions of jammed traffic. In fact, we have observed isolated jams in the corresponding spatiotemporal plots of the traffic density. For a density of 35 vehicles/km, the diagram indicates regions of free, synchronized, and jammed traffic, while free traffic is observed for densities of 25 vehicles/km and below.

The time-headway distributions for $\rho=35$ vehicles/km and 40 vehicles/km shown in Fig. 7(b) are essentially equivalent to those for the open system, see Fig. 3(a). Notice that the height of the peak of the distribution for free traffic (in contrast to that for congested traffic) depends strongly on the initial conditions and the duration of the simulations. Therefore, the observed quantitative difference in this aspect does not weaken our conclusion.

Finally, in Fig. 7(c), we show the variation coefficient resulting from the simulation. The comparison with Fig. 1(c) displays a nearly quantitative agreement for densities below 30 vehicles/km, and a qualitative one for higher densities.

In summary, we have found that the statistical properties of the closed system are essentially the same as those of the open system in regions of comparable density, and that a circular road can serve as a test bed for the VDT mechanism. As a consequence, an on-ramp is not needed to produce the typical effects of VDT models as described in Secs. IV A and IV B.

V. DISCUSSION

In the variance-driven time headway model put forward in this paper, the desired safety time headway is a dynamic variable increasing with the local velocity variance. This provides a mechanism for a spontaneous formation and decay of long-lived but nonpermanent platoons: If traffic flow is stable, initial velocity differences decrease, leading to decreased values of the local variance and thereby to low values of the desired time headway and a high dynamic road capacity. Because of the conservation of the vehicle number, this automatically leads to platoons and to large gaps in front of the slowest vehicles (trucks). For sufficiently high traffic demands the short time gaps may result in unstable traffic flow, leading to higher values of the variance. This, in turn, causes spontaneous braking maneuvers of the drivers which further increase the velocity variance. Finally, this breaks up the whole platoon resulting in a traffic breakdown with a distinct capacity drop.

Our intention is to propose a simple model for this variance-driven mechanism. Therefore, we have neglected, e.g., finite reaction times or more elaborated concepts of anticipation which are contained, for example, in the human driver model (HDM) [14]. Furthermore, we have modeled fluctuations in the simplest possible way. Moreover, we restricted ourselves to single-lane traffic.

In the following, we want to discuss our main results in the light of the VDT mechanism.

(i) The distribution of time headways in free traffic is broad and asymmetric both in the deterministic and stochastic cases, although all vehicles (cars and trucks) have the same time-headway parameter. The reason is that the time headway depends dynamically on the velocity variance. Consequently, even the deterministic driver-vehicle units do not have a unique fundamental diagram.

(ii) The averaged time headway in congested traffic is almost 2 times that in free traffic (Figs. 1 and 3), which is related to the higher values of the velocity variation coefficient for congested traffic compared to free traffic.

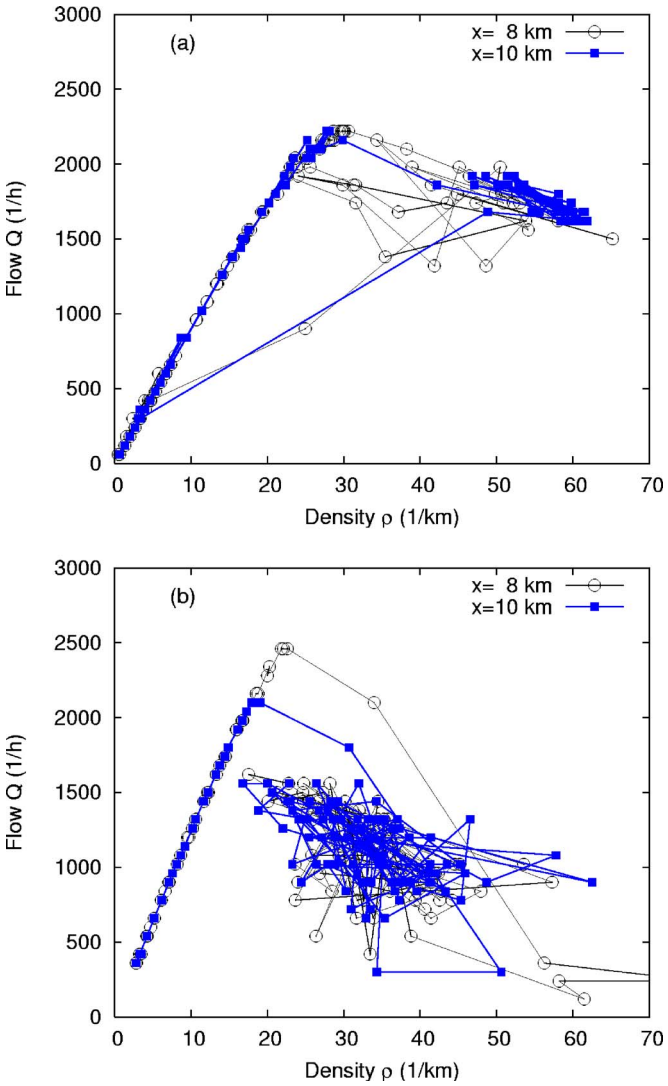

FIG. 8. (Color online) Effects of heterogeneity vs VDT effects on the fundamental diagram. The plots show the simulation scenario of Fig. 6(a) with the following changes: (a) without VDT modification, i.e., using the IDM directly for cars and trucks; (b) VDT-IDM with identical vehicles (cars).

(iii) On a macroscopic level, the VDT reproduces the wide scattering of data points in the flow-density diagram calculated from 1-minute data, and the capacity drop at the transition from free to congested traffic [Fig. 6(a)].

Notice that some statistical properties of single-vehicle data are expected to depend strongly on the distinction between single-lane and multilane traffic. This is particularly true for the distributions of times-to-collision (TTC), $\tau_\alpha^{\mathrm{TTC}}=s_\alpha/(v_\alpha-v_{\alpha-1})$. On a single-lane road with very restricted or nonexistent overtaking possibilities, the faster cars queue behind the slowest vehicles (trucks), so eventually all vehicles drive at nearly the same velocity leading to higher TTC values and therefore to a narrower distribution of the relative approaching rates compared to multilane roads. Since we are not aware of traffic data for single-lane traffic, we did not include TTC into this paper.

In presenting our simulation results, we have emulated the available data analogously to real traffic data. For example,

we did not use the full information of all vehicle trajectories for determining the times-to-collision. Instead, we have restricted ourselves to virtual detectors, as this approach allows a *direct* comparison with empirical traffic data.

To separate the VDT effects from possible effects of heterogeneous traffic or noise, we run several VDT simulations with and without noise for a mixture of cars and trucks and for cars alone. Furthermore, we simulated the underlying models directly, i.e., without the VDT modifications. All these simulations showed that the proposed results such as the time-headway statistics, the capacity drop, and the wide scattering in the fundamental diagram (Fig. 8) are genuine effects of the VDT mechanism, which are only slightly modified by heterogeneity or noise. Moreover, most of the proposed results cannot be reproduced with heterogeneity and/or noise alone. In order to show that the perturbations induced by merging traffic at the on-ramp do not play a significant role, we plotted all results for two locations $x=10$ km (near the ramp), and $x=8$ km (2 km further upstream). Since we found no big differences at these two locations, we conclude that perturbations induced by mergings play a minor role. This is confirmed by our simulations for the ring-road scenario.

We note that an understanding of the effects of the velocity variance is crucial for devising measures to avoid traffic breakdowns: The VDT feedback mechanism is triggered most likely near sources of sustained velocity variations, for example, in the merging, diverging, or weaving zones near freeway intersections, but also the noise term plays a role as can be seen in the fundamental diagrams discussed in Sec. IV B. These simulations show that it is essential to avoid merging and diverging maneuvers at high velocity differences, e.g., by increasing the length of the acceleration lane at on-ramps and off-ramps. Another measure to reduce the velocity variance are speed limits which can be simulated with the VDT as well. Furthermore, since lane changes constitute another source of velocity variance, we expect a strong coupling of lane changes to the longitudinal dynamics by the VDT mechanism. In particular, multilane simulations with the VDT mechanism [33] and empirical distributions of the time gaps T_0 are expected to yield a fully quantitative explanation of bottleneck effects introduced by weaving zones and off-ramps, and also a quantitative explanation of the observed TTC statistics on multilane roads.

Finally, the distinct increase of the time headways after traffic breakdown opens up vehicle-based options to increase traffic performance and stability by means of adaptive cruise control (ACC) systems. Such driver-assistance systems, which accelerate and brake automatically depending on the distance to the preceding vehicle and its velocity, are already commercially available for some upper-class vehicles. By a suitable strategy for varying the time headways of ACC systems as a function of the traffic situation, the unfavorable human behavior can be partially compensated for. First simulations of such ACC systems show promising results [34,35].

ACKNOWLEDGMENTS

The authors would like to thank the Volkswagen AG within the BMBF project INVENT for partial support.

[1] B. Tilch and D. Helbing, in *Traffic and Granular Flow '99*, edited by D. Helbing, H. Herrmann, M. Schreckenberg, and D. Wolf (Springer, Berlin, 2000), pp. 333–338.
[2] L. Neubert, L. Santen, A. Schadschneider, and M. Schreckenberg, Phys. Rev. E **60**, 6480 (1999).
[3] B. S. Kerner and H. Rehborn, Phys. Rev. E **53**, R4275 (1996).
[4] K. Nishinari, M. Treiber, and D. Helbing, Phys. Rev. E **68**, 067101 (2003).
[5] B. S. Kerner, *The Physics of Traffic* (Springer, Heidelberg, 2004).
[6] D. Helbing, Rev. Mod. Phys. **73**, 1067 (2001).
[7] W. Knospe, L. Santen, A. Schadschneider, and M. Schreckenberg, Phys. Rev. E **65**, 056133 (2002).
[8] M. Treiber, A. Hennecke, and D. Helbing, Phys. Rev. E **59**, 239 (1999).
[9] M. M. Minderhoud and P. H. L. Bovy, Accid. Anal Prev. **33**, 89 (2001).
[10] S. Hirst and R. Graham, in *Ergonomics and Safety of Intelligent Driver Interfaces*, edited by Y. Noy (Lawrence Erblaum Associates, New Jersey, 1997).
[11] F. Hall and K. Agyemang-Duah, Transp. Res. Rec. **1320**, 91 (1991).
[12] C. Daganzo, M. Cassidy, and R. Bertini, Transp. Res., Part B: Methodol. **33**, 25 (1999).
[13] B. S. Kerner and H. Rehborn, Phys. Rev. Lett. **79**, 4030 (1997).
[14] M. Treiber, A. Kesting, and D. Helbing, Physica A **360**, 71 (2006).
[15] H. Lenz, C. Wagner, and R. Sollacher, Eur. Phys. J. B **7**, 331 (1999).
[16] M. Treiber and D. Helbing, Phys. Rev. E **68**, 046119 (2003).
[17] L. Neubert, L. Santen, A. Schadschneider, and M. Schreckenberg, in *Traffic and Granular Flow '99*, edited by D. Helbing, H. Herrmann, M. Schreckenberg, and D. Wolf (Springer, Berlin, 2000), pp. 307–314.
[18] M. Treiber and D. Helbing, cond-mat/9901239 (unpublished).
[19] P. G. Gipps, Transp. Res., Part B: Methodol. **15**, 105 (1981).
[20] M. Brackstone and M. McDonald, Transportation Research Part F **2**, 181 (1999).
[21] K. Nagel and M. Schreckenberg, J. Phys. I **2**, 2221 (1992).
[22] W. Knospe, L. Santen, A. Schadschneider, and M. Schreckenberg, Phys. Rev. E **70**, 016115 (2004).
[23] B. S. Kerner and S. L. Klenov, J. Phys. A **35**, L31 (2002).
[24] P. Wagner, cond-mat/0411066 (unpublished).
[25] M. Treiber and D. Helbing, J. Phys. A **32**, L17 (1999).
[26] D. Helbing and M. Treiber, Cooper@tive Tr@nsport@tion Dyn@mics 1, 2.1 (2002) (Internet Journal, www.TrafficForum.org/journal).
[27] M. Bando, K. Hasebe, A. Nakayama, A. Shibata, and Y. Sugiyama, Phys. Rev. E **51**, 1035 (1995).

[28] R. Jiang, Q. Wu, and Z. Zhu, Phys. Rev. E **64**, 017101 (2001).
[29] M. Treiber, A. Hennecke, and D. Helbing, Phys. Rev. E **62**, 1805 (2000).
[30] D. Chowdhury, L. Santen, and A. Schadschneider, Phys. Rep. **329**, 199 (2000).
[31] D. Helbing and M. Treiber,Physica A **363**, 62 (2006).
[32] C. Gardiner, *Handbook of Stochastic Methods* (Springer, New York, 1990).
[33] M. Treiber and D. Helbing, in *ASIM 2002*, edited by D. Tavangarian and R. Grützner (Tagungsband 16, Symposium Simulationstechnik, Rostock, 2002), pp. 514–520.
[34] M. Treiber and D. Helbing, Automatisierungstechnik **49**, 478 (2001).
[35] A. Kesting, M. Treiber, M. Schönhof, F. Kranke, and D. Helbing, *Traffic and Granular Flow '05* (Springer, Berlin, 2006).